第 49 卷第 8 期
2021 年 8 月

硅 酸 盐 学 报
JOURNAL OF THE CHINESE CERAMIC SOCIETY

Vol. 49，No. 8
August，2021

http://www.gxyb.cbpt.cnki.net

DOI：10.14062/j.issn.0454-5648.20200926

综 合 评 述

用原位透射电镜技术观察微晶玻璃结晶过程的研究进展

王 婷[1,3]，高 伟[3]，余 雪[2]，周大成[2]，邱建备[2]，徐旭辉[2]，余兆丰[3]

(1. 成都理工大学材料与化学化工学院，成都 610051；2. 昆明理工大学材料科学与工程学院，昆明 650093；
3. 香港理工大学应用物理系，香港 999999)

摘 要：总结了利用原位透射电子显微镜(TEM)技术观察纳米颗粒在玻璃介质中结晶过程的研究进展。原位 TEM 技术可以提供一个实时记录纳米颗粒形核结晶以及长大的动力学平台，该技术为理解和优化微晶玻璃中纳米颗粒生长机理提供了方法，从而为实现优化纳米颗粒结晶性、形貌以及其物理特性提供了直接途径。此外，还总结了微晶玻璃中纳米颗粒的成核机理，详细讨论了温度和电子束(E-beam)对纳米颗粒在玻璃介质中生长动力学过程的影响，并提出了原位 TEM 技术在微晶玻璃材料中应用的机遇和挑战。

关键词：原位透射电子显微镜；微晶玻璃；结晶；纳米颗粒；生长过程；电子束
中图分类号：TQ175　　**文献标志码**：A　　**文章编号**：0454–5648(2021)08–1559–08
网络出版时间：2021–07–20



Crystallization Behavior of Glass Ceramics by *in-situ* Transmission Electron Microscopy - A Short Review

WANG Ting[1,3], *GAO Wei*[3], *YU Xue*[2], *ZHOU Dacheng*[2], *QIU Jianbei*[2], *XU Xuhui*[2], *YU Siufung*[3]
(1. Chengdu University of Technology, College of Materials and Chemistry & Chemical Engineering, Chengdu 610051, China;
2. Kunming University of Science and Technology, College of Materials Science and Engineering, Kunming 650093, China;
3. Department of Applied Physics, The Hong Kong Polytechnic University, Hong Kong 999999, China)

Abstract: Recent work on the characterization of nanoparticles crystallization process in glassy matrix by *in-situ* transmission electron microscopy (TEM) was represented. *In-situ* TEM technique as an effective tool can determine the structural dynamics of nanoparticles in real-time to clarify and optimize their structures and properties. We summarized the dynamic process stages of glass ceramics growth, *i.e*., phase separation, nucleation, crystallization and coalescence. The electron beam (E-beam) and thermal effects on the nanoparticle growth process in glassy matrix were discussed. In addition, the opportunities and challenges of *in-situ* TEM applied to glass ceramics were also proposed.

Keywords: *in-situ* transmission electron microscopy; glass ceramic; crystallization; nanoparticles; growth; E-beam

1 Introduction

Glass ceramic as at least one type of functional crystalline phase and residual glass is fabricated *via* controlled crystallization of glass with different compositions in various processing methods[1]. The properties of glass ceramics can be modulated in various aspects, such as mechanical, chemical, optical, and thermal properties, which are depended on the microstructure, size, morphology, and distribution of nanoparticles in vitreous glassy matrix. Glass ceramics are applied to abrasion materials, crystallization glaze in space and electronic industries due to their unique characteristics[2–4]. Recent work reported the upconversion

收稿日期：2020–12–23。　修订日期：2021–02–22。
基金项目：国家自然科学基金(61775187, 61965012)。
第一作者：王 婷(1991—)，女，博士，研究员。
通信作者：邱建备(1970—)，男，博士，教授。
徐旭辉(1986—)，男，博士，教授。

Received date: 2020–12–23.　**Revised date:** 2021–02–22.
First author: WANG Ting (1991–), female, Ph. D., Researcher.
E-mail: wangtkm@foxmail.com
Correspondent author: QIU Jianbei (1970–), male, Ph. D., Professor;
XU Xuhui (1986–), male, Ph. D., Professor.
E-mail: qiu@kmust.edu.cn; xuxuh07@126.com

luminescence of rare-earth element doped oxyfluoride glass ceramic, which can realize the conversion from infrared light to visible light[5–6]. This glass ceramic has great potential applications in visible light solid-state lasers or other fields, and becomes a research hotspot worldwide. Since a suitable crystalline phase with a proper microstructure is critical for obtaining desirable optical properties, chemical and thermal stabilities, it is thus rather important to control and optimize the crystallization process of nanoparticles. Clarifying the kinetics growth process of nanoparticles in glassy system is thus considered as one of the most important steps for designing the desired properties of glass ceramics.

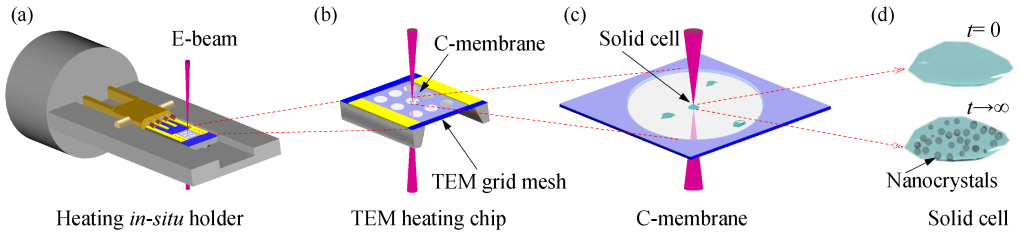
In-situ TEM has attracted much attentions recently. It can provide a platform to record the structural dynamics process of nanoparticles [7–9]. Therefore, it is necessary to clarify the formation of glass ceramic by using *in-situ* TEM. In this paper, we represented the design and the development of *in-situ* TEM for the characterization of glass ceramic, and discussed the crystallization behavior of nanoparticles of glass ceramic[10]. Besides, the universality of *in-situ* TEM by varying molar compositions was highlighted. We summarized the E-beam and thermal effects on the nanoparticle growth process. In addition, we also provided a challenge for future development and application of *in-situ* TEM applied to glass ceramics.

2 Design and fabrication of amorphous glass by *in-situ* TEM technique

Glass can be fabricated by using glass melting methods, *i.e.*, raw materials with different molar compositions are mixed and melted at a high temperature, and then the melted mixture is poured out to form amorphous glass. Amorphous glass needs to be ground into the finer size to obtain *in-situ* TEM images. Figure 1 shows the diagram of *in-situ* TEM measurement for glass ceramics. In Fig. 1b, amorphous glass is dispersed with alcohol on a carbon membrane of a heating chip. In Fig. 1a, the heating chip is then installed by a heating holder after alcohol is evaporated. The nanoparticles can be emerged in glassy matrix to form glass ceramics during *in-situ* TEM measurement due to the thermal annealing or E-beam irradiation. There are some advantages of using a glassy matrix to observe the nanoparticles growth by *in-situ* TEM, such as high-temperature operation (>180 °C), high spatial resolution, high temporal resolution and compaction with a conventional TEM system [10].

Glasses have little change in a high vacuum environment, and can withstand at a high temperature, so using an amorphous glass to determine the crystallization behavior is thus easily manipulated. Besides, glassy matrix can provide a high temporal resolution without the use of ultrafast recording devices because atoms have a low diffusion rate in glassy matrix rather than in liquid. Furthermore, glass has a higher tolerance to ionize the radiation damage rather than liquid. The nucleation and crystallization rates can be controlled to realize high-resolution (HR) *in-situ* TEM recording. The *in-situ* TEM for the observation of nanoparticles growth in a glassy matrix can present a stale growth process with a high spatial and temporal resolution, showing that the detailed transition dynamic of the nanocrystal formation from glass matrix can be recorded in a long irradiation period.

Table 1 shows the operation parameters for amorphous glass with different material compositions. Clearly, ZnO, $CsPbBr_3$, Ba_2LaF_7 and Ag represent oxide, perovskite, semiconductor and metal materials, respectively, which are selected to demonstrate the universality of *in-situ* TEM measurement on amorphous glass. Our group also used *in-situ* TEM to observe Ba_2LaF_7 nanoparticles growth and coalescence in $45SiO_2$–$15Al_2O_3$–$12Na_2O$–$21BaF_2$–$7LaF_3$ glass. In our work, $45SiO_2$–$15Al_2O_3$–$12Na_2O$–$21BaF_2$–$7LaF_3$ glass ceramic was firstly heated at 680 °C to form Ba_2LaF_7 nanoparticles under atmospheric condition[10], showing that Ba_2LaF_7 nanoparticles could be obtained in the glass composition, and then the amorphous glass ($45SiO_2$–$15Al_2O_3$–$12Na_2O$–$21BaF_2$–$7LaF_3$) was dispersed at heating chips for *in-situ* TEM measurement. Also, Ba_2LaF_7 nanoparticles could be formed at an E-beam irradiation of 2.7 A/cm^2 and a heating temperature of 500 °C. The success of *in-situ* TEM measurement of Ba_2LaF_7 nanoparticles indicates that the amorphous glass can act under the growth condition to support the nanoparticles formation. Subsequently, ZnO, Ag and perovskite nanoparticles can be also formed due to the E-beam and thermal effects. In Table 1, the heating temperature and E-beam intensity are modulated for different materials and compositions [11–12].



(a) Heating chip is loaded by TEM heating chip, (b) TEM heating chip deposits with amorphous glass, (c) Enlarged heating chip, and (d) micro-diagram of an amorphous glass before and after thermal annealing and E-beam irradiation.

Fig. 1 Diagram of *in-situ* TEM measurement for glass ceramics

Table 1　Operation parameters for glass ceramics with different material compositions

Sample	Molar Compositions	*T* (in atmosphere)	NP (1)	*T* (*In-situ* TEM)	NP (2)
1	$40SiO_2$-$10Al_2O_3$-$15K_2O$-35ZnO	780 °C	ZnO	750°C+2.7A/cm^2	ZnO
2	$45SiO_2$-$15Al_2O_3$-$12Na_2O$-$21BaF_2$-$7LaF_3$	680 °C	Ba_2LaF_7	500°C+2.7A/cm^2	Ba_2LaF_7
3	$65B_2O_3$-$8Al_2O_3$-$27Na_2O$-Ag_2O	300 °C	Ag	RT+2.7A/cm^2	Ag
4	6ZnO-$3SrCO_3$-$9Cs_2O$-$3PbBr_2$-6NaBr	500 °C	$CsPbBr_3$	RT+2.7A/cm^2	$CsPbBr_3$

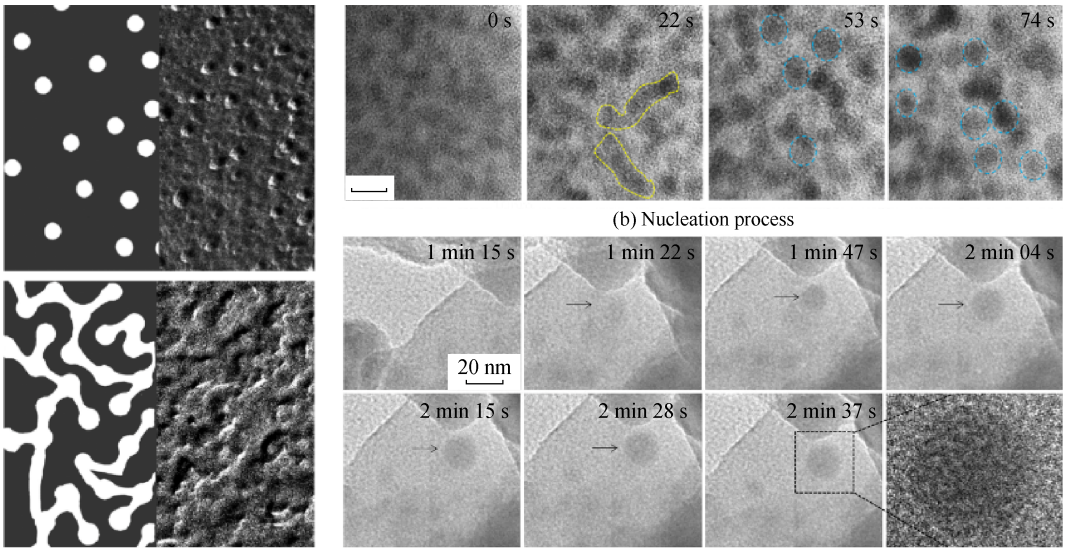
RT — Room temperature; *T* — Temperature; NP (1) — Nanoparticles formed in atmosphere; NP (2) — Nanoparticles formed by *in-situ* TEM.

3　Growth process of nanoparticles in glassy matrix

Investigating the nanoparticle crystallization mechanism in glassy matrix can solve one of the basic scientific issues in a glass ceramic. Because the formation dynamic, nanoparticle size/morphology, and crystalline property of glass ceramic can be modulated for the optimization of its corresponding physical properties. A recent work[12] used *in-situ* TEM to investigate the formation dynamic of ZnO nanoparticles in glassy matrix in atomic scale. The results indicate that high spatial and temporal resolutions of the TEM observation provide a possibility for understanding the growth mechanism, diffusion, and coalescence process of glass ceramic. The nanoparticles formation in glassy matrix is augmented *via* improvement in a resolution under the effects of thermal and E-beam energies, allowing a greater range of synthesis techniques to be addressed. Glass ceramic formation process involves the glass molecular structure, amorphous phase separation and crystallization process.

3.1　Nucleation process of glass ceramic

Nucleation process is a key factor controlling the crystallization process, and it is a first step in the formation of either a thermodynamic phase or a structure by self-organization or self-assemble process[13–15]. Russel *et al* reported the interpenetration phase separation and their compositional evolution by TEM[16]. They reported that the size and phase of crystals in glassy matrix can be controlled by the initial phase separation. Figure 2a shows their results, which reported that the crystallization behavior can be changed by modulating the glasses compositions of xKF−$x$$ZnF_2$−(100–2$x$)$SiO_2$ oxyfluoride glass. When the compositional threshold of x is 20% and 22.5% in glassy matrix, glass compositions with two thresholds concentrations have two different microstructures, showing different phase separations and compositional evolutions in glassy systems. It is concluded that the nanoparticle size and crystal phase (*i.e.*, K_2SiF_6 and $KZnF_3$) of glass ceramic can be modulated *via* the initial phase separation.



(a) TEM　　(b) Nucleation process　　(c) *In-situ* TEM

Fig. 2　Nucleation of nanoparticles in glassy matrix

In our recent work[11–12], *in-situ* TEM technique was used to determine the nucleation process with different nanoparticles, *e.g.* $CsPbBr_3$, ZnO. Figure 2b, shows the nucleation process of $CsPbBr_3$ in $34B_2O_3$–$3SiO_2$–8ZnO–3SrO–$8Cs_2O$–3PbBr–6NaBr glassy matrix. The results show that the nucleation process of $CsPbBr_3$ nanoparticles at E-beam irradiation includes phase separation, aggregation and finally formation of $CsPbBr_3$ nanoclusters. The initial TEM image of glassy matrix appears at 0 s. The phase separation occurs as the

irradiation time prolongs (at 22 s). At 53 s, the nucleation and growth processes occur. Also, the similar nucleation also appears in ZnO glass ceramic with the glass composition of $40SiO_2$–$10Al_2O_3$–$15K_2O$–35ZnO. Figure 2c shows the *in-situ* TEM image of the initial nucleation stage of a ZnO amorphous nanocluster in glassy matrix. At 75 s, there is no phase separation and aggregation in the process. At 7 s, the formation of ZnO-rich phase separation occurs. As a result, a nanocluster with a diameter of ~15 nm appears and eventually grows to ~22 nm in diameter at 82 s. This multi-step growth mechanism also occurs in nanoparticles growth process inside the liquid cell measured by *in-situ* TEM[5–17], indicating that the growth mechanism of the nanoparticles in glassy matrix is similar to that of the nanoparticles in liquid.

3.2 Crystallization process of glass ceramics

Some reports show that it is necessary to distinguish the homogeneous and heterogeneous nucleation processes in the glassy crystal formation [18–21]. According to the homogeneous nucleation theory, a phase appears without any external boundary due to the local fluctuation of density and kinetic energy. For the heterogeneous nucleation process, foreign boundaries, such as substrates and grain boundaries, are involved. Heterogeneous nucleation typically occurs in glass ceramics because foreign boundaries cannot exclude, and is important in the development of glass ceramics [22–24]. During the TEM observation, there is no direct observation of the crystallization mechanism of the glass ceramic. The heterogeneous nucleation process is recorded firstly in glass ceramics by *in-situ* TEM. Figure 3a shows the *in-situ* high resolution TEM images of a ZnO nanoparticle at E-beam intensity of 10.8×10^4 A/m^2 and heating temperature of 750 °C. The transformation of ZnO crystals from the amorphous state to the crystalline state is clearly shown. The crystal phase emerges initially from the amorphous cluster interface by prolonging the irradiation time, and then the crystallization process is completed at 554 s. Figure 3b shows the *in-situ* high resolution TEM images of an Ag nanoparticle in glassy matrix. Like the growth mechanism of ZnO nanoparticle, the growth process of Ag nanoparticles also emerges from the interface of the Ag amorphous cluster. Finally, at 39 s, the entire nanocluster is consumed, and the size of Ag nanoparticle becomes ~8 nm [12]. It is thus demonstrated that the heterogeneous nucleation process can be observed in glass ceramics with the nanoparticles emerged initially from the cluster interface (interface can act as a foreign boundary). The transition from the amorphous state to the crystalline state in glass ceramics can be attributed to the high viscosity of glass ceramics. Figure 3c shows the crystallization mechanism diagram of nanoparticles in glassy matrix. The initial crystallization process at the interface of the nanocluster is the linkage between nanocluster and the nanocrystals. Hence, the use of amorphous-to-crystalline phase transition to connect the direct and indirect multistep pathways is due to the coexistent growth mechanisms of glass ceramics [25].

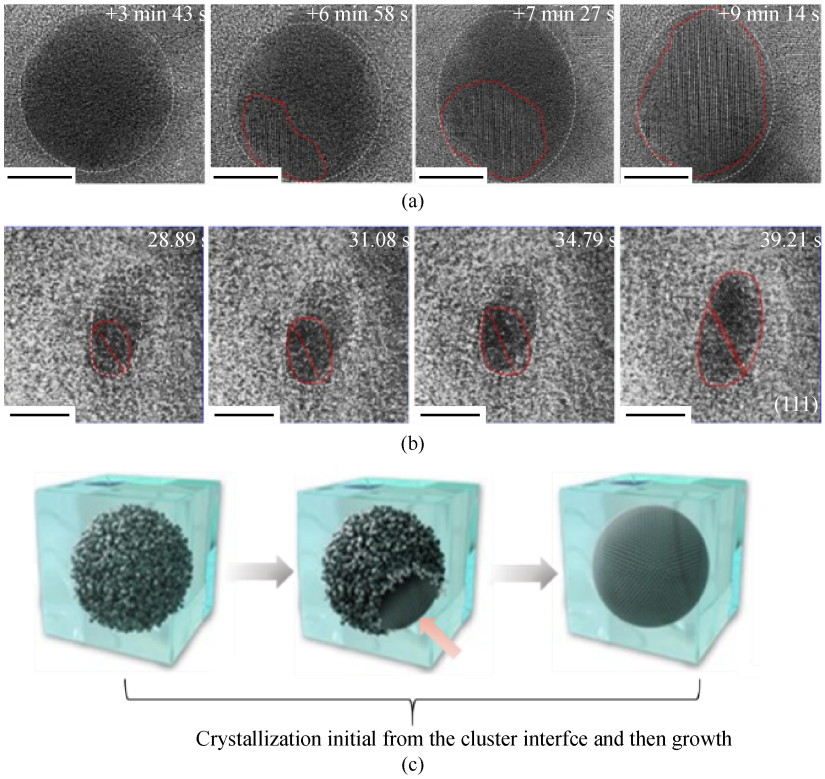


Fig. 3 *In-situ* TEM images of (a) ZnO and (b) Ag nanoparticles crystallization process in glassy matrix and (c) crystallization mechanism of glass ceramics

3.3 Coalescence process of glass ceramics

Coalescence process can control the material properties because the material has tunable properties with respect to their composition, size and shape[26]. According to the classical theory, nanoparticles coalescence process often involves the orientation attachment and Ostwald ripening[27–29]. Therefore, understanding the fundamental mechanism of coalescence process could favor to guide the modulation of the nanoparticles structure for effective properties. The coalescence of the nanoparticles in glassy matrix is also investigated by *in-situ* TEM, including the orientation attachment and Ostwald ripening processes. Figure 4a shows Ba_2LaF_7 nanoparticles in $45SiO_2$–$15Al_2O_3$–$12Na_2O$–$21BaF_2$–$7LaF_3$ glass compositions. Clearly, there are two Ba_2LaF_7 nanocrystals with different crystallographic orientations[10]. The two nanocrystals enjoy a coalesce process and the misoriented lattice fringes join at a boundary to form a single Ba_2LaF_7 nanocrystal at the irradiation time of 40 s. The larger nanocrystal grows through the consumption of the boundary atoms of smaller nanocrystal and finally forms the single defect-free particles with continuously increasing the irradiation time.

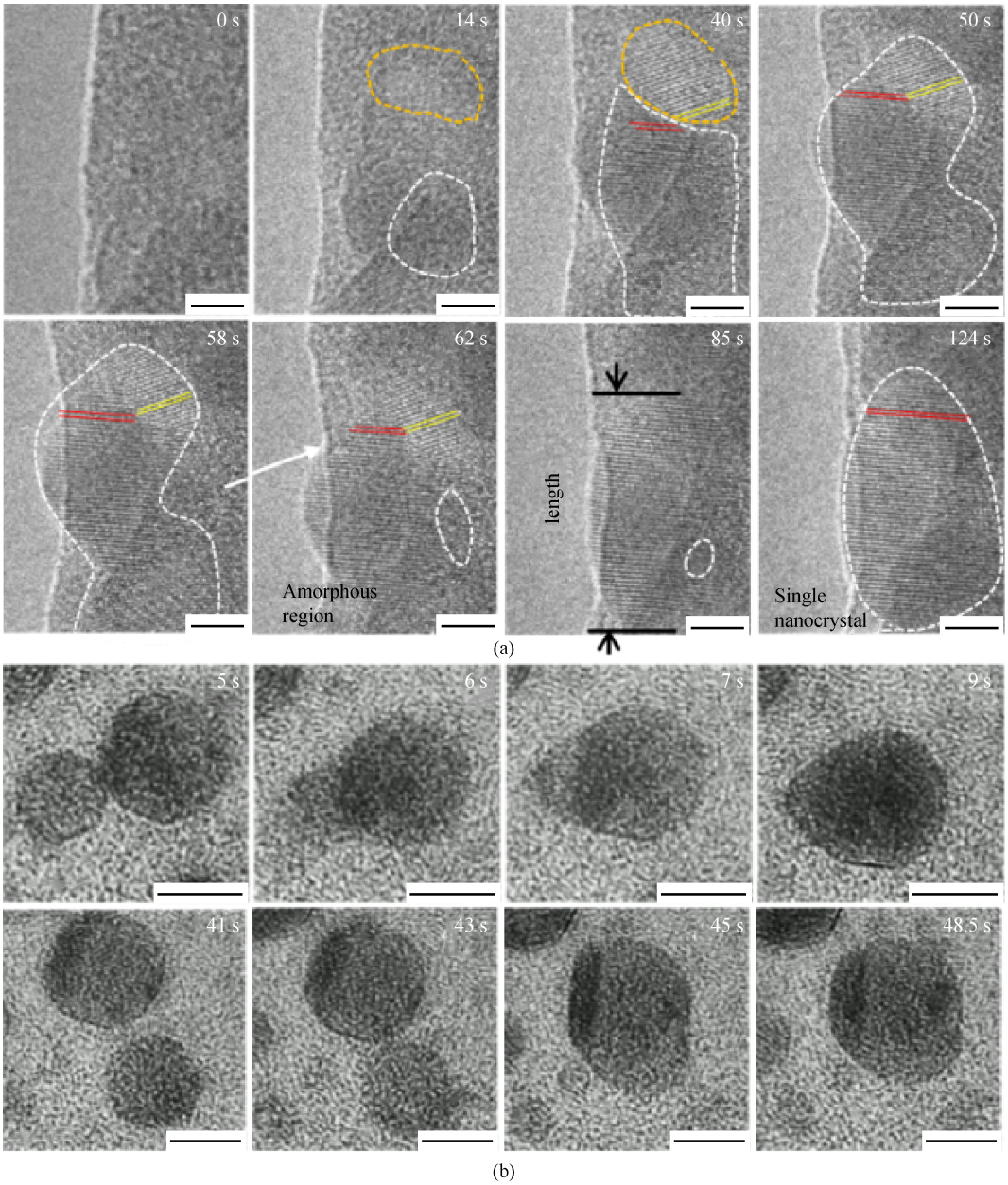


Fig. 4　Coalescence process of Ba_2LaF_7 nanoparticles (a) and $CsPbBr_3$ nanoparticles (b) in the glass ceramics

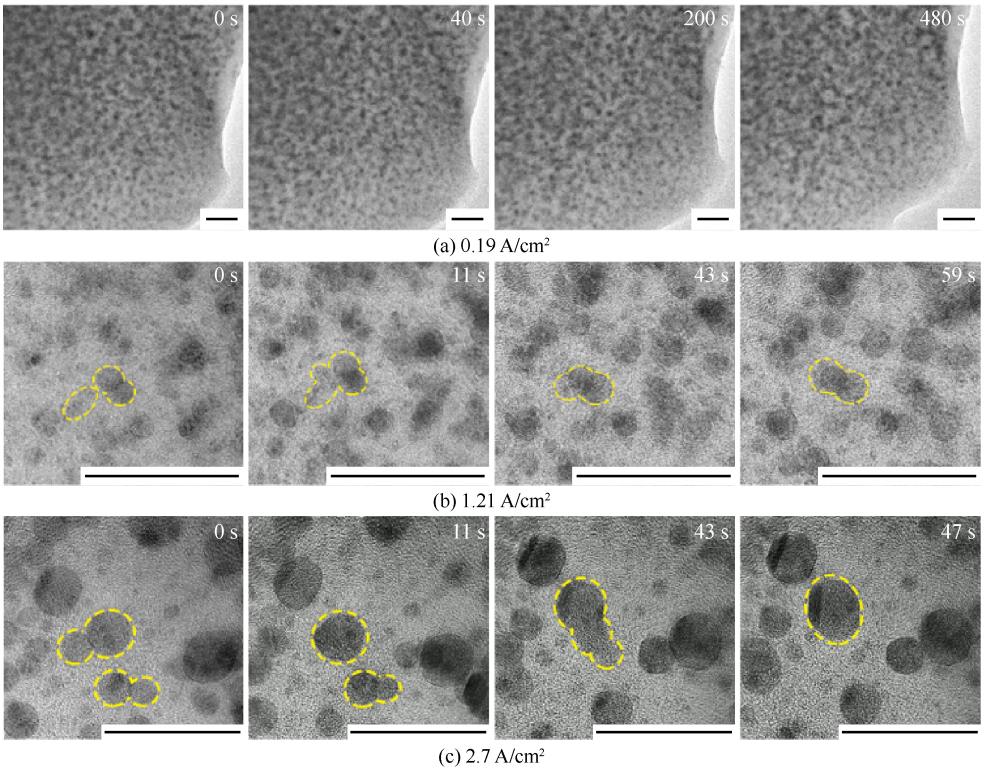
Figure 4b shows two $CsPbBr_3$ nanoparticles in $34B_2O_3$–$3SiO_2$–$8ZnO$–$3SrO$–$8Cs_2O$–$3PbBr$–$6NaBr$ glass compositions [11]. The Ostwald ripening involved with the smaller particle is melted immediately once it touches the larger one and then grows by monomer attachment with migrating atoms towards the larger one. It is thus summarized that the coalescence process for glass ceramics is a resemble process, and it can provide a

relatively high spatial resolution so that we can observe the coalescence process clearly, particularly for the coalescence process in the initial stage and the boundary movement during the orientation attachment process.

4 E-beam irradiation and thermal effect on glass ceramics

4.1 E-beam irradiation in nanoparticles growth process

A highly focused E-beam can be used to induce the atoms diffusion and manipulate nanoparticles movement rate to observe nanoparticles dynamic mechanism [30–32]. The understanding of constructive and destructive interactions of high energy E-beam with the sample material can guide the nanoparticles growth process and clarify the chemical or physical reaction mechanism. There are many reports regarding E-beam adjusting the nanoparticles growth and movement (*i.e.*, electron tweezers) to probe the interaction between the nanoparticles and the growth environment while observing the dynamic mechanism of nanoparticles motion. [33] A previous study reported that the E-beam can be used for the modulation of gold nanoparticles formation rate in liquid. The results showed that the trapping force of the E-beam can be directly detected and measured by the probability distribution of gold nanoparticles [34–35]. As for the E-beam effect on glass ceramic, our previous work also demonstrated that the E-beam effect on glassy matrix has the similar phenomenon, compared to that on liquid. Figure 5 shows the *in-situ* TEM images of perovskite glass ceramics at different E-beam irradiation intensities.[11] Clearly, the coalescence occurs slowly when the E-beam intensity is below 2.7 A/cm^2. $CsPbBr_3$ nanoparticles coalescence occurs dramatically when the E-beam intensity increases to 2.7 A/cm^2. E-beam can trigger the nanoparticles growth process, but it can damage the nanoparticles. Although there is no decomposition from the glass ceramics under E-beam irradiation, the decomposition effect cannot be ignored. Nevertheless, the nature of the E-beam effect on the glass ceramics is complex and still need to be further investigated.



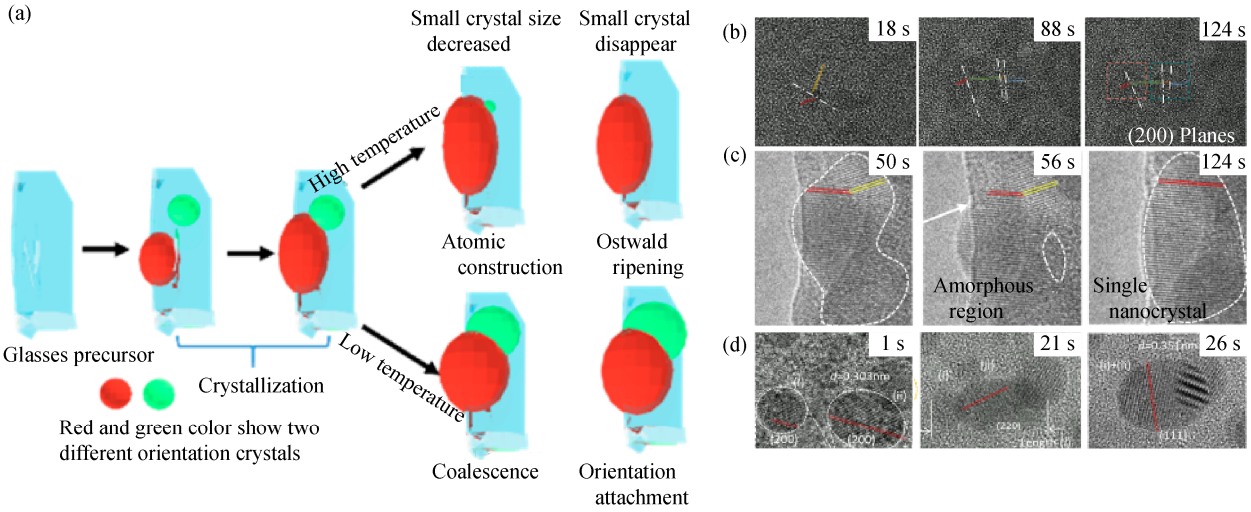
Scale bar is 10 nm.

Fig. 5 *In-situ* TEM images of perovskite glass ceramics at different E-beam irradiation intensities

4.2 Thermal effect in nanoparticles growth process

Thermal energy can induce nanoparticles nucleation, growth, and coalescence processes according to the thermodynamic models. Therefore, nanoparticles can be adjusted flexibly with a desirable microstructure as the heating temperature is increased [36]. In a previous work[10], heating effect on the growth of the nanoparticles in glass ceramic was investigated. The results showed that coalescence of Ba_2LaF_7 nanocrystals can be modulated flexibly by controlling the heating temperature, as shown in Fig. 6. Clearly, Ba_2LaF_7 nanoparticles with the absence of defects (twinned and quadruplet) are formed at a relatively low temperature (*i.e.*, ≤430 °C), and the unification of two nanocrystals

via the two pathways (*i.e.*, migration with and without rotation) is obtained when the heating temperature is increased (*i.e.*, ≥470 °C). The defect-free single Ba_2LaF_7 nanocrystal can be formed because a higher temperature can provide a higher thermal energy, and then trigger the reconstruction and recrystallization processes.



(a) Mechanism of the thermal effect on the ceramic glasses; *in-situ* TEM image of the Ba_2LaF_7 coalescence process at different temperature, (b) 430 ºC, (c) 470 ºC, (d)500 ºC.

Fig. 6　Thermal effect of the ceramic glasses

5　Conclusion and perspective

In-situ TEM provides unique information for recording glass ceramics formation and transformation process with high spatial and temporal resolution. It can provide significant opportunities to record nanoparticles nucleation, growth, and coalescence dynamic processes in glassy matrix. The liquid cells require thin and strong windows to isolate the aqueous solution in a high vacuum environment. Compared to liquid cells, glassy matrix has little influence in a high vacuum environment, and can withstand at a high temperature. The *in-situ* TEM is thus easy to be manipulated. A high temporal and spatial resolution can be obtained simultaneously from the high resolution TEM images due to the slow diffusion rate and high transparency of glassy matrix. For the growth mechanism, the detailed growth dynamics of the nanoparticles in glassy matrix can be recorded in detail. The phase separation, nucleation, crystallization, and coalescence are observed with a high resolution. Particularly, the observation of the amorphous-to-crystalline phase transition can connect the direct and indirect multistep pathways due to the coexistent growth mechanisms of non-classical nucleation theory.

During *in-situ* TEM observation, heating can provide the thermal energy to trigger the nanoparticles growth process in glassy matrix. Once an amorphous glass is fabricated in glass-manufacturing process, a solid-state glass has a high viscosity (>10^6 dPa·s), impeding the atom migration to nucleation and growth. Crystallization is hardly achieved because quenching glass-manufacturing process in a short time cannot provide sufficient time for the growth, and even if the precipitated nucleus appears. Therefore, the amorphous glass in the absence of precipitated nanoparticles is obtained. Once the amorphous glass is heated at a suitable temperature, thermal annealing can provide thermal activation, significantly triggering the formation of the nanoparticles. Therefore, TEM heating chip can be used to preciously control the heating temperature of glass ceramics and then contribute to the modulation of the growth behavior.

In fact, for *in-situ* TEM, the E-beam is often used as an energy source to trigger the reaction. The high energy E-beam can induce the diffusion, decomposition of glass ceramics composition, so the nanoparticles growth can occur when the dose of E-beam exceeds the threshold. Although some previous studies showed that the growth of nanoparticles under an E-beam is similar to that under a flask, it is difficult to qualitatively and quantitatively analyze the relationship between the E-beam intensities and growth mechanism under *in-situ* TEM vacuum condition. This is because the E-beam can induce the formation of nanoparticles initially, and trigger the side reactions, as well as the reaction between the E-beam and sample is complex. High energy electrons generate primary and secondary radiation products. Moreover, the E-beam triggers different reactions in different samples, and these effects can be complex and difficult to be predicted. In the future, more efforts are needed to make a breakthrough in the E-beam effect on glass ceramic formation process during *in-situ* TEM measurement.

References:

[1] VIVIANE O S, FRANCISCO C S, GABRIEL S O, et al. Highly translucent nanostructured glass-ceramic[J]. Ceram Int, 2021, 47(21): 4707–4714.

[2] BEALL G. Design and properties of glass-ceramics[J]. Annual Rev Mater Sci, 1992, 22(1): 91–119.

[3] RICHERSON D W. Modern Ceramic Engineering: Properties, Processing, and Use in Design[M]. CRC Press: 2005.

[4] AXINTE E. Glasses as engineering materials: A review[J]. Mater Design, 2011, 32(4): 1717–1732.

[5] CHEN D, WANG, YU Y, et al. Novel rare earth ions-doped oxyfluoride nano-composite with efficient upconversion white-light emission[J]. J Solid State Chem, 2008, 181(10): 2763–2767.

[6] LI Z, ZHOU D, YANG Y, et al. Adjustable multicolor up-energy conversion in light-luminesce in Tb^{3+}/Tm^{3+}/Yb^{3+} co-doped oxyfluoride glass-ceramics containing Ba_2LaF_7 nanocrystals[J]. Scient Rep, 2017, 7(1): 1–11.

[7] LIU D, SHADIKE Z, LIN R, et al. Review of recent development of in situ/operando characterization techniques for lithium battery research[J]. Adv Mater, 2019, 31(28): 1806620.

[8] GROGAN J M, BAU H H. The nano aquarium: a platform for in situ transmission electron microscopy in liquid media[J]. J Microelectromech Systems, 2010, 19(4):885–894.

[9] YUAN Y, AMINE K, LU J, et al. Understanding materials challenges for rechargeable ion batteries with in situ transmission electron microscopy[J]. Nat Commun, 2017, 8(1): 1–14.

[10] WANG T, LU W, XU X, et al. Study of Crystallization and coalescence of nanocrystals in amorphous glass at high temperature[J]. Inorg Chem, 2019, 58(14): 9500–9504.

[11] WANG T, YANG Z, YANG L, et al. Atomic-scale insights into the dynamics of growth and degradation of all-inorganic perovskite nanocrystals[J]. J Phys Chem Lett, 2020, 11(12): 4618–4624.

[12] WANG T, LU W, YANG Q, et al. In situ observation of nucleation and crystallization of a single nanoparticle in transparent media[J]. J Phys Chem C, 2020, 124(28): 15533–15540.

[13] RINCÓN J M. Principles of nucleation and controlled crystallization of glasses[J]. Polymer-Plastics Technol Eng, 1992, 31(3/4): 309-357.

[14] BREU J, SEIDL W, HUTTNER D, et al. Nucleation-controlled crystallization of a new, spontaneously resolved solvate of [Ru $(bpy)_3$]$(PF6)_2$ and its desolvation reaction[J]. Chemistry–A Eur J, 2002, 8(19): 4454–4460.

[15] WOEHL T J, EVANS J E, ARSLAN I, et al. Direct in situ determination of the mechanisms controlling nanoparticle nucleation and growth[J]. ACS Nano, 2012, 6(10): 8599–8610.

[16] LIN C, BOCKER C, RÜSSEL C. Nanocrystallization in oxyfluoride glasses controlled by amorphous phase separation[J]. Nano Lett, 2015, 15(10): 6764–6769.

[17] NIELSEN M H, ALONI S, DE YOREO J J. In situ TEM imaging of $CaCO_3$ nucleation reveals coexistence of direct and indirect pathways[J]. Science, 2014, 345(6201): 1158–1162.

[18] YINNON H, UHLMANN D R. A kinetic treatment of glass formation V: surface and bulk heterogeneous nucleation[J]. J Non-Cryst Solids, 1981, 44(1): 37–55.

[19] HÖLAND W, RHEINBERGER V, SCHWEIGER M. Control of nucleation in glass ceramics[J]. Philoso T R Soc A, 2003, 361(1804): 575–589.

[20] MILEVA D, ANDROSCH R, ZHURAVLEV E, et al. Homogeneous nucleation and mesophase formation in glassy isotactic polypropylene[J]. Polymer, 2012, 53(2): 277–282.

[21] GEBERT A, ECKERT J, SCHULTZ L. Effect of oxygen on phase formation and thermal stability of slowly cooled $Zr_{65}Al_{7.5}Cu_{17.5}Ni_{10}$ metallic glass[J]. Acta mater, 1998, 46(15): 5475–5482.

[22] SHI Y, LI B W, ZHAO M, et al. Growth of diopside crystals in CMAS glass-ceramics using Cr_2O_3 as a nucleating agent[J]. J Am Ceram Soc, 2018, 101(9): 3968–3978.

[23] LOFGREN G E. Effect of heterogeneous nucleation on basaltic textures: a dynamic crystallization study[J]. J Petrol, 1983, 24(3): 229–255.

[24] DA N, PENG M, KROLIKOWSKI S, et al. Intense red photoluminescence from Mn^{2+}-doped (Na^+; Zn^{2+}) sulfophosphate glasses and glass ceramics as LED converters[J]. Opt Exp, 2010, 18(3): 2549–2557.

[25] SARKIES K, FRANKEL N. Nonclassical nucleation theory[J]. Phys Rev A, 1975, 11(5): 1724.

[26] MANDAL M, GHOSH S K, KUNDU S, et al. UV photoactivation for size and shape controlled synthesis and coalescence of gold nanoparticles in micelles[J]. Langmuir, 2002, 18(21): 7792–7797.

[27] CAO D, GONG S, SHU X, et al. Preparation of ZnO nanoparticles with high dispersibility based on oriented attachment (OA) process[J]. Nanoscale Res Lett, 2019, 14(1): 210.

[28] RIBEIRO C, LEE E J, LONGO E, et al. A kinetic model to describe nanocrystal growth by the oriented attachment mechanism[J]. Chem Phys Chem, 2005, 6(4): 690–696.

[29] BALDAN A. Review progress in Ostwald ripening theories and their applications to nickel-base superalloys Part I: Ostwald ripening theories[J]. J Mater Sci, 2002, 37(11): 2171–2202.

[30] DYCK O, KIM S, JIMENEZ-IZAL E, et al. Building structures atom by atom via electron beam manipulation[J]. Small, 2018, 14(38): 1801771.

[31] DE JONGE N, ROSS F M. Electron microscopy of specimens in liquid[J]. Nat Nanotechnol, 2011, 6(11): 695–704.

[32] TAHERI M L, STACH E A, ARSLAN I, et al. Current status and future directions for in situ transmission electron microscopy[J]. Ultramicroscopy, 2016, 170: 86–95.

[33] LIAO H-G, ZHENG H. Liquid cell transmission electron microscopy[J]. Annual Rev Phys Chem, 2016, 67: 719–747.

[34] Zheng H. Using molecular tweezers to move and image nanoparticles[J]. Nanoscale, 2013, 5(10): 4070–4078.

[35] ZHENG H, MIRSAIDOV U M, WANG L W. Electron beam manipulation of nanoparticles[J]. Nano Lett, 2012, 12(11): 5644–5648.

[36] THANH N T, MACLEAN N, MAHIDDINE S. Mechanisms of nucleation and growth of nanoparticles in solution[J]. Chem Rev, 2014, 114(15): 7610–7630.